

Effect of thermal curing on Ni speciation: information from XAS spectra

Hui-Chin Huang^a, Yu-Ling Wei^{a,*}, Yao-Wen Yang^b, Jyh-Fu Lee^b

^a Department of Environmental Science, Tunghai University, Taichung 407, Taiwan

^b National Synchrotron Radiation Research Center, Hsinchu 300, Taiwan

Available online 25 February 2005

Abstract

This study applied X-ray absorption spectroscopy (XAS) to investigate the change in molecular environment of nickel in clay after 2-h thermal curing at 500–1100 °C.

The main peak at the edge of the 900 and 1100 °C XANES spectra shifts toward higher photon energy (i.e., about +1.5 eV) compared with the 105 and 500 °C sample XANES. The intensity of main peak at the edge increases with curing temperature. These information leads to the inference of highly distortion of Ni(II) environment in the 900 and 1100 °C cured samples, which is not observed in the Ni XANES spectra of the 105 and 500 °C samples. The shift of multiple scattering feature indicates the change in the geometry of the medium range structure around Ni target element after thermal curing. EXAFS evidence indicated that Ni crystallite size increased with higher curing temperature.

© 2005 Elsevier B.V. All rights reserved.

Keywords: Clay; Ni XANES; Multiple scattering; China; Sorbent

1. Introduction

Clay is a valuable resource that can be used as an important raw material for manufacturing industries of firebrick/brick. Ni has frequently been studied in various fields using X-ray absorption spectroscopy (XAS) [1–3]. It has many useful applications in our life and is harmful if discharged into the environment [4]. Nickel contaminant can cause various adverse health effects to human [5].

Synchrotron-based XAS, including X-ray absorption near-edge structure (XANES) and extended X-ray absorption fine structure (EXAFS), is capable of revealing scientific issues such as speciation, distribution, reactivity, form transformations, mobility, and bioavailability of trace metal contaminants [6]. XAS has been employed for metal speciation [7–9] and for molecular level studies of trace metal in contaminated soils, realistic soil analogue sorbents, and organics [10–19].

The objective of this research is to investigate the effect of thermal curing on nickel molecular environment in clay with usage of XAS technique.

2. Materials and method

The clay was pre-dried at 105 °C for 3–5 days. The dried clay was ground and sieved to less than 50 mesh. To prepare the artificially nickel-contaminated clay, slurry containing 1.5 l of 198.13 g Ni(NO₃)₂·6H₂O solution and 1.0 kg clay was end-to-end rotated in a bottle at a speed of 30 rev/min for 2 days. The mixed slurry was then dried at 105 °C in an electric oven for 3 days. The nickel content doped in dried clay was 40,000 mg Ni²⁺ (kg clay)⁻¹. The dried sample was then ground to less than 50 mesh and ready for thermal curing at 500–1100 °C in an electrically heated oven for 2 h. After the curing process, the sample was discharged, cooled, and stored from moisture for Ni XAS spectrum recording.

Ni K-edge (8333 eV) XAS spectra were recorded on wiggler C (BL-17C) beamline at the National Synchrotron Radiation Research Center (NSRRC) of Taiwan. The ring storage energy was 1.5 GeV, the beam current was 120–200 mA. The span of the monochromator in the beamline was 4–15 keV, and the energy resolution ($\Delta E/E$) was 1.9×10^{-4} . All spectra were recorded in transmission mode at room temperature. The references were NiO, Ni₂O₃, Ni(NO₃)₂·6 H₂O, and Ni(OH)₂. WinXAS 3.0 software [20] was employed for data reduction.

* Corresponding author. Tel.: +886 4 23591368; fax: +886 4 23596858.
E-mail address: yulin@mail.thu.edu.tw (Y.-L. Wei).

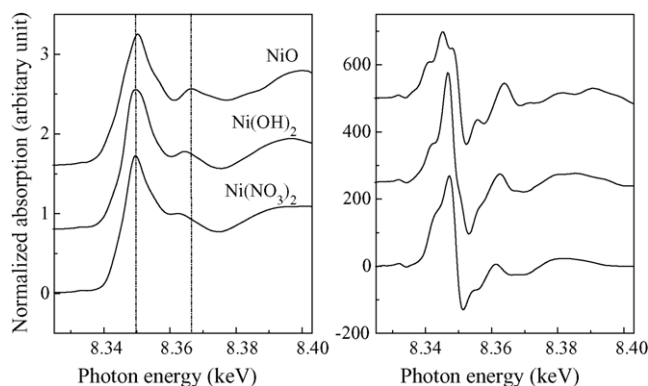


Fig. 1. XANES (left) and their first derivative spectra (right) of reference nickel compounds.

3. Result and discussion

The left column of Fig. 1 shows the XANES spectra of reference compound NiO, Ni(OH)₂, and Ni(NO₃)₂·6H₂O. All reference Ni XANES spectra have the pre-edge peak at photon energy of ca. 8335 eV due to the electron transition to empty d orbital. Its intensity is extremely low. The main edge (feature B in Fig. 1) is similar for the references. There is a slight shift in the multiple scattering feature (feature C) that is associated with geometry of the medium range structure among the references [21]. The corresponding derivative spectra of references, presented in the right column of Fig. 1, are different from each other.

Fig. 2 shows the XANES spectra (left column) and their corresponding derivative spectra (right column) of heated samples. All sample XANES spectra have the pre-edge feature showing the electron transition to empty d-orbital. Feature B, the main peak at the edge, of the 900 and 1100 °C XANES spectra shifts toward higher photon energy (i.e., about +1.5 eV) compared with the 105 and 500 °C sample XANES. However, a close examination of the 900 and 1100 °C XANES spectra in feature B shows that there is a

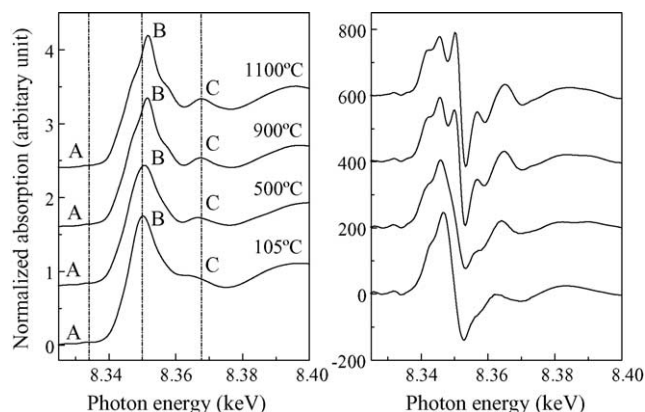


Fig. 2. XANES (left) and their first derivative spectra (right) of Ni-containing clay after drying at 105 °C for 3–5 days or thermal curing at 500–1100 °C for 2 h.

shoulder towards the edge jump, which can be explained by a highly distorted Ni(II) environment.

The intensity of feature B increases with thermal curing temperature. On the other hand, the distortion of Ni(II) environment is not observed in the 105 and 500 °C samples. There is a slight shift of feature C toward greater photon energy for samples cured at higher temperature. This suggests the change in the geometry of the medium range structure around Ni target element after thermal curing. The XANES derivative spectra (right column of Fig. 1) show considerably difference from each other. The height of peaks occurred at 8350 and 8357 eV are greater in the 900 and 1100 °C spectra than that in the 105 and 500 °C spectra.

Fig. 3 depicts the Fourier transforms (solid curve) and their corresponding fitted spectra (open circle curve) from references and samples. NiO and Ni(OH)₂ show a complex structure due to the higher long-range order around nickel. In contrast, the structure of the Fourier transform of Ni(NO₃)₂·6H₂O is very simple, indicating a lack of long-range order. It is noted that Ni(NO₃)₂·6H₂O reference is a salt with six hydrated water molecules and is monoclinic.

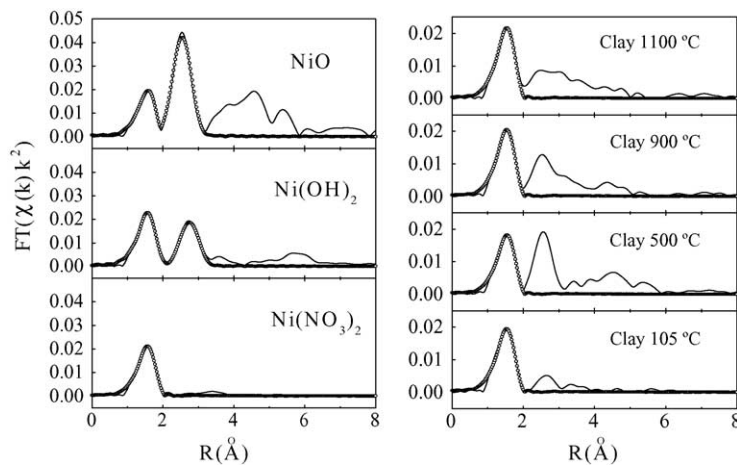


Fig. 3. Fourier transforms of EXAFS spectra of reference nickel compounds (left) and thermally cured samples (right).

Table 1
Structural parameters of reference nickel compounds

Sample	1st shell		2nd shell	
	$N_{1st\ shell}$ at R (Å)	σ^2 (Å ²)	$N_{2nd\ shell}$ at R (Å)	σ^2 (Å ²)
Ni(NO ₃) ₂ ·6H ₂ O ^a	5.50 Ni–O at 2.05	0.0045	b	b
Ni(OH) ₂ ^c	6.00 Ni–O at 2.05	0.0047	6.00 Ni–Ni at 3.13	0.0054
NiO ^a	6.00 Ni–O at 2.08	0.0055	12.0 Ni–Ni at 2.94	0.0053

^a Based on NiO crystallographic data.

^b No second shell.

^c Based on Ni(OH)₂ crystallographic data.

The structural parameters resulting from the fitting of Fourier transforms of reference compounds are listed in Table 1. Single-shell fitting is performed over 0.9–2.1 Å range for Ni(NO₃)₂·6H₂O and two-shell fitting in 0.9–3.1 Å range for NiO and Ni(OH)₂. The first shell and the second shell are, respectively, occupied by oxygen and nickel atoms. The first shell interatomic distance is similar for all references. However, Ni(OH)₂ shows longer second shell interatomic distance than NiO does. The Debye–Waller factor for all references is relatively similar to each other, in 0.0045–0.0055 Å² range.

The right column of Fig. 3 shows the fitting of Fourier transforms of nickel-containing clay samples dried at 105 °C or thermally cured at 500–1100 °C. Only the 500 °C sample shows a complex structure. Curing at higher temperature results in simpler structure in Fourier transform spectrum. The 900 and 1100 °C samples show that the second shell is not well resolved from the third shell.

Table 2 lists the structural parameters resulting from the single shell fitting of the Fourier transforms of cured samples by fixing the Debye–Waller factor at 0.0055 Å² based on the results from fitting NiO reference (see Table 1). The structural results for the 105 °C sample are similar to that for the Ni(NO₃)₂·6H₂O reference shown in Table 1, that is consistent with the XANES results. The first-shell coordination number increases with increasing curing temperature in the 500–1100 °C range, possibly indicating increased sintering effect and thus greater nickel compound crystallite size at higher temperature. In spite of the difference in curing temperature, the first-shell interatomic distance is invariable for all thermally cured samples.

Table 2
Structural parameters of Ni(II)-containing clay after drying at 105 °C for 3–5 days or thermal curing at 500–1100 °C for 2 h

Sample (°C)	1st shell	
	$N_{1st\ shell}$ at R (Å)	σ^2 (Å ²)
105 ^a	5.55 Ni–O at 2.03	0.0055
500 ^a	5.20 Ni–O at 2.04	0.0055
900 ^a	5.73 Ni–O at 2.03	0.0055
1100 ^a	6.09 Ni–O at 2.03	0.0055

^a Based on NiO crystallographic data.

4. Conclusion

The edge of the main peak in the XANES spectra for samples cured at 900 and 1100 °C shifts toward higher photon energy (i.e., about +1.5 eV), compared with the 105 and 500 °C sample XANES, and there is an increase in the intensity of the main peak at the edge with higher curing temperature. This suggests that Ni(II) environment is highly distorted in the 900 and 1100 °C cured samples. The nickel in the samples treated at 105 and 500 °C is almost entirely in a form of Ni(NO₃)₂·6H₂O and Ni(OH)₂, respectively.

Higher curing temperature in 500–1100 °C range results in a decreased long-range molecular order around Ni in the clay samples. It is suggested that curing at higher temperature enhanced nickel compound crystallite size, possibly due to a greater sintering effect.

Acknowledgments

We thank the staff of NSRRC of Taiwan for their assistance in the XAS experiment.

References

- [1] Y. Uchimoto, H. Sawada, T. Yao, J. Power Sources 97–98 (2001) 326.
- [2] D.M. Bhardwaj, D.C. Jain, S. Dalela, R. Kumar, N.L. Saini, K.B. Garg, Physica B 350 (2004) 366.
- [3] M. Sun, T. Bürgi, R. Cattaneo, D. van Langeveld, R. Prins, J. Catalysis 201 (2001) 258.
- [4] K. Kadirvelu, M. Kavipriya, C. Karthika, M. Radhika, N. Vennilamani, S. Pattabhi, Bioresour. Technol. 87 (2003) 129.
- [5] R.P. Beliles, in: F.W. Oehme (Ed.), Toxicity of Heavy Metals in the Environment, Part 2, Marcel Dekker, New York, 1979, p. 383.
- [6] U.S. Department of Energy. Report of DOE Molecular Environmental Science Workshop, 5–8 July 1995. Airlie Center, VA.
- [7] T.K. Tokunaga, S.R. Sutton, S. Bajt, P. Nuessle, G. Shea-McCarthy, Environ. Sci. Technol. 32 (1998) 1092.
- [8] M.D. Szulczewski, P.A. Helmke, W.F. Bleam, Environ. Sci. Technol. 31 (1997) 2954.
- [9] A.J. Francis, C.J. Dodge, F. Lu, G.P. Halada, C.R. Clayton, Environ. Sci. Technol. 28 (1994) 636.
- [10] M. Dyar, D. Delaney, J.S. Sutton, S.R. Schaefer, W. Martha, Am. Miner. 83 (1998) 1361.
- [11] A. Manceau, M.C. Boisset, G. Sarret, J.J. Hazemann, M. Mench, P. Cambier, R. Prost, Environ. Sci. Technol. 30 (1996) 1540.

- [12] L. Charlet, A. Manceau, J. Colloid Interface Sci. 148 (1992) 425.
- [13] A. Manceau, P.R. Buseck, D. Miser, J. Rask, D. Nahon, Am. Miner. 75 (1990) 490.
- [14] A. Manceau, L. Charlet, M.C. Boisset, B. Didier, L. Spadini, Appl. Clay Sci. 7 (1992) 201.
- [15] A. Manceau, L. Charlet, J. Colloid Interface Sci. 168 (1994) 87.
- [16] L. Spadini, A. Manceau, P.W. Schindler, L. Charlet, J. Colloid Interface Sci. 168 (1994) 73.
- [17] G. Sarret, A. Manceau, D. Cuny, C.V. Haluwyn, S. Deruelle, J.L. Hazemann, Y. Soldo, L. Eybert-Berard, J.J. Menthonnex, Environ. Sci. Technol. 32 (1998) 3325.
- [18] K.F. Hayes, A.L. Roe, G.E. Brown Jr., K.O. Hodgson, J.O. Leckie, G.A. Parks, Science 238 (1987) 783.
- [19] G.V. Korshin, A.I. Frenkel, E.A. Stern, Environ. Sci. Technol. 32 (1998) 2699.
- [20] T. Ressler, J. Synchrotron Rad. 5 (1998) 118.
- [21] L. Galoisy, L. Cormier, G. Calas, V. Briois, J. Non-Crystalline Solids 105 (2001) 293.